ISSN 0915-633X

NIFS--209

JP9306166

NATIONAL INSTITUTE FOR FUSION SCIENCE

Density Dependence of Line Intensities and Application to Plasma Diagnostics

K. Masai

(Received – Jan. 20, 1993)

NIFS-209

Feb. 1993

NAGOYA, JAPAN

DENSITY DEPENDENCE OF LINE INTENSITIES AND APPLICATION TO PLASMA DIAGNOSTICS

Kuniaki MASAI

National Institute for Fusion Science, Nagoya 464-01, Japan

ABSTRACT

Electron density dependence of spectral lines are discussed in view of application to density diagnostics of plasmas. The dependence arises from competitive level population processes, radiative and collisional transitions from the excited states. Results of the measurement on tokamak plasmas are presented to demonstrate the usefulness of line intensity ratios for density diagnostics. Also general characteristics related to density dependence are discussed with atomic-number scaling for H-like and He-like systems to be helpful for application to higher density plasmas.

Keywords: excitation, line emission, density dependence

Send proofs to: Kuni MASAI
Service d'Astrophysique
CEN Saclay
F-91191 Gif-sur-Yvette Cedex
FRANCE
(from 01/02/93 through 01/02/94)

1. Introduction

Spectroscopy of radiation from a hot plasma is of practical importance for diagnostics as well as of interest in atomic physics of highly charged ions. Spectra of various species in a plasma give information not only of their abundances and ionization states but of the electron temperature and the density of the plasma. The temperature and the density can be obtained also by other means, e.g. Thomson scattering in tokamak plasmas. It may be stressed that the temperature and the density obtained from line spectra reflect straightforward the environment of the ion in the thermal structure of the plasma.

Atomic processes for the electron temperature and the density diagnostics are so simple as to be applied easily for various configurations of atomic structure. We here give a basic concept for the electron density measurements by use of line spectra. The density dependence of line intensities (specific intensities) comes from the competition of radiative decay and collisional transitions from the excited level. At a low density limit, the population of the excited levels are negligible compared to the ground state since excitation is followed immediately by radiative decay to lower levels without collision. Then the line intensity is in proportion to the rate of excitation from the ground state. With increasing the electron density, collisional transitions from the excited state to other upper levels become significant and take over the radiative decay to lower levels. At a high density limit, the population is dominated by collisional processes to be a Boltzmann distribution, as in a thermodynamic equilibrium. Then, the line intensity can be given by the radiative transition probability and the Boltzmann factor. In the intermediate region between the two limits, the specific intensity naturally exhibits the electron density dependence.

We have studied the density dependence of line intensities of oxygen and iron in tokamak plasmas. Some examples of these observations are presented with discussion of the applicability to density diagnostics. In the following section, we give a simple account for the electron density dependence of line intensities. In section 3, metastable levels of Be-like oxygen and B-like iron are discussed with an application to the density diagnostics of tokamak plasmas. In the final section, some remarks on the density dependence are presented for H-like and He-like systems.

2. Principle of density dependence

Line intensity is proportional to the population of the excited state, which is determined by a couple of equations of all the transitions among all the energy levels. In addition, transitions from/to another ion have to be taken into account when the ionization state is far from the equilibrium. However, the problem much reduces for two extreme cases; the electron density is much smaller or higher than the radiative transition probability divided by the rate coefficient of the competitive collisional process. At a high density limit, collisional de-excitation dominates the transitions from excited states and the level population is ruled by a Boltzmann distribution. On the other hand, at a low density limit, radiative decay dominates the transitions from excited states and the population of excited states are negligibly small compared to that of the ground state. This condition of population is often called corona after the condition attained for solar corona.

In order to give a simple account for the density dependence of line intensities, we consider a schematic two-level atom consisting of levels 1 and 2, the ground state and the excited state, respectively. With level k representing all other upper levels including the free electron state, a couple of rate equations for the level population of the atom can be written as,

$$\begin{aligned} \frac{\mathrm{d}\, n_1}{\mathrm{d}\, t} &= - n_e(C_{12}+C_{1k})n_1 + n_e C_{21} n_2 + n_e C_{k1} n_k + A_{21} n_2, \\ \frac{\mathrm{d}\, n_2}{\mathrm{d}\, t} &= n_e C_{12} n_1 - n_e(C_{21}+C_{2k})n_2 + n_e C_{k2} n_k - A_{21} n_2, \end{aligned} \tag{1}$$

where n_j represents the population of the level j, n_e the electron density, and C_{ij} and A_{ij} represent the rate coefficient for electron-impact excitation and the radiative transition probability from the level i to j, respectively. Generally, the rate coefficient C_{ij} can be expressed as a function of the electron temperature T_e independently of n_e. In some practical situations, collisional transition by particles other than electrons may be important. Here, however, only the collision by electrons is considered. With a stationary state, eq. (1) gives populations of the levels 1 and 2 as,

$$\frac{n_2}{n_1} = \frac{n_e C_{12} + n_e C_{1k} C_{k2}/(C_{k1}+C_{k2})}{A_{21} + n_e C_{21} + n_e C_{2k} C_{k1}/(C_{k1}+C_{k2})} \approx \frac{n_e C_{12}}{A_{21} + n_e C_{21}}, \tag{2}$$

where the last expression means a 2-level atom approximation and may be attained practically when the plasma is neither ionizing nor recombining.

At the low density limit as $n_e \ll A_{21}/C_{21}$, $n_2/n_1 \approx n_e C_{12}/A_{21}$ and the population of the excited state is negligibly small. Then the line intensity of the transition from the level 2 to 1 can be given by

$$I_{21} \approx A_{21} n_2 \approx n_e C_{12} n_1 \approx n_e C_{12} n, \tag{3}$$

in proportion to the rate of excitation from the ground state, and the density of the ion in its ground state n_1 is nearly equal to the ion density n. In this situation, radiative transition probability plays no explicit roles for line intensities. The collisional transition rate to optically forbidden (non E1) levels is smaller than that to optically allowed levels by only a factor, yet the corresponding radiative transition rate is smaller by several orders of magnitude. Therefore, under a corona condition as described by eq. (3), forbidden lines can be observed with considerable intensities much higher than those expected straightforward from their radiative transition probabilities.

With Maxwell distribution of electrons, the rate coefficient for excitation from a level i to j can be written generally in a form

$$C_{ij}(T_e) = G_{ij}\, T_e^{-(1/2+\alpha_{ij})}\, e^{-E_{ij}/kT_e}, \tag{4}$$

where $G_{ij} \equiv \langle G(kT_e/E_{ij}) \rangle$ is an extended Gaunt factor averaged over the Maxwellian, E_{ij} is the transition energy and α_{ij} is a parameter depending on the transition i to j; $\alpha \approx 0$ for electric dipole (E1) transitions and generally $\alpha > 0$ for non E1 transitions. Any line exhibits a dependence of its intensity simply proportional to the electron density. Intending to discuss the specific density dependence of line intensities, we compare the

intensities of two lines to eliminate the trivial density dependence. Using eq. (4), we can obtain an expression for the line intensity ratio at the low density limit, as

$$I_{ji}/I_{ki} = C_{ij}/C_{ik} = (G_{ij}/G_{ik})\ T_e^{-(\alpha_j-\alpha_k)}\ e^{-(E_j-E_k)/kT_e} \approx (G_{ij}/G_{ik})\ e^{-(E_j-E_k)/kT_e}, \qquad (5)$$

where the last expression can be attained for the ratio of E1 transition lines. The exponential T_e dependence with weak T_e dependence of G_{ij}/G_{ik} gives an account for temperature diagnostics by use of resonance-series lines with much different excitation energies or the different principal quantum numbers of the excited states. Eq. (5) is independent of the electron density and gives an asymptotic value toward the low density limit. In the corona regime, the line intensities are determined by the direct excitation from the ground state, and their relative intensities are to be a function only of the electron temperature.

With increasing the electron density, $n_e C_{21}$ becomes significant compared to a constant A_{21} in eq. (2). At the high density limit as $n_e \gg A_{21}/C_{21}$, the population of the two-level atom is given by $n_2/n_1 \approx C_{12}/C_{21} \approx (g_2/g_1)\ e^{-E_{12}/kT_e}$ as the result of the detailed balancing between excitation and de-excitation by collision, where g_1 and g_2 are the statistical weight. Thus the line intensity can be written as

$$I_{21} \approx A_{21}\ n_2 \approx \frac{g_2}{g_1} e^{-E_{12}/kT_e} A_{21}\ n_1 \approx \frac{(g_2/g_1)\ e^{-E_{12}/kT_e}}{1 + (g_2/g_1)\ e^{-E_{12}/kT_e}} A_{21}\ n, \qquad (6)$$

independently of the electron density. Thus the intensity ratio of two lines at the high density limit can be written in a form

$$I_{ji}/I_{ki} \approx (g_j/g_k)\ (A_{ji}/A_{ki})\ e^{-(E_j-E_k)/kT_e}. \qquad (7)$$

The intensity ratio of two lines or the relative intensities of lines must vary from a value given by eq. (5) at the low density limit to a value given by eq. (7) at the high density limit with increasing the electron density.

The schematic behavior of the line intensity ratio is shown in Fig. 1 as a case that the ratio increases with increasing the density. Regions (i) and (iii) correspond to the corona and the Boltzmann regimes, respectively, where the ratio is close to the respective constants at the two limits. In the intermediate density region denoted by (ii), the intensity ratio varies to be applicable to density diagnostics. The critical densities dividing these three regimes depend on the radiative decay probabilities of the excited states concerned. In a tokamak plasma, the corona condition is attainable for resonance series lines, but not always for the lines associated with metastable levels such as forbidden lines. Further excitation to other upper levels can occur by electron impact from excited levels of small radiative decay probabilities even at low densities, whereas the resonance lines immediately follow the excitation from the ground state with much larger radiative decay probabilities. Then the intensity ratio of the former line to the resonance line can be a measure of the electron density.

3. Practical applications to density diagnostics

As an example, the atomic level configuration of Be-like oxygen (O V) is shown in Fig. 2. At low densities, excitation to 2s2p (^{3}P) metastable state is followed by radiative decay to the $2s^2$ (^{1}S) ground state into a line at 1218 A. As the density increases, collisional excitation from 2s2p (^{3}P) state to $2p^2$ (^{3}P) is enhanced to result in the line 2s2p (^{3}P) - $2p^2$ (^{3}P) at 760 A, while the line $2s^2$ (^{1}S) - 2s2p (^{3}P) becomes less prominent relatively to the resonance line. This situation is seen in Fig. 3 (a), where the relative intensities of the above two lines to the resonance line $2s^2$ (^{1}S) - 2s2p (^{1}P) are shown as a function of the electron density.[1] These lines are practically prominent and sensitive at densities lower than 10^{13} cm^{-3}, which may be attained for the peripheral region of tokamaks[2]. Fig. 3 (b) shows a similar calculation[3], where the behavior of the ratio 2s2p (^{3}P) - $2p^2$ (^{3}P) to the resonance line is different from one in Fig. 3 (a) at lower densities. This difference is mainly due to taking direct excitation from the ground state into account for the population of $2p^2$ (^{3}P) state in Fig. 3 (b). As a result the intensity ratio exhibits a reasonable asymptotic behavior toward the corona limit, as suggested by the discussion in section 2 and Fig. 1.

Another example is shown in Fig. 4 for B-like iron with a doublet ground state. At

low densities, $2s^22p$ ($^2P_{1/2}$) is substantially populated, and the line intensity ratio of $2s^22p$ ($^2P_{3/2}$) - $2s2p^2$ ($^2P_{3/2}$) 114 A to $2s^22p$ ($^2P_{1/2}$) - $2s2p^2$ ($^2S_{1/2}$) 117 A is determined by the ratio of the rates of excitation to $2s2p^2$ ($^2P_{3/2}$) and $2s2p^2$ ($^2S_{1/2}$) from $2s^22p$ ($^2P_{1/2}$) state. With increasing the electron density, population of $2s^22p$ ($^2P_{3/2}$) increases and the excitation to $2s2p^2$ ($^2P_{3/2}$) therefrom is enhanced to take a place of excitation from $2s^22p$ ($^2P_{1/2}$) for $2s^22p$ ($^2P_{3/2}$) - $2s2p^2$ ($^2P_{3/2}$) line at high densities. With a 4-level atom, the intensity ratio of the two lines can be expressed as,

$$\frac{I_{42}}{I_{31}} \approx \frac{b_{42}}{b_{31}}\left(\frac{C_{14}}{C_{13}} + \frac{C_{24}}{C_{13}}\frac{n_2}{n_1}\right), \tag{8}$$

where

$$b_{jk} = A_{jk}/(\sum_i A_{ji} + n_e \sum_i C_{ji})$$

is the branching ratio for the radiative transition from level j to level k. In the corona regime, the second term is negligible compared to the first one in the bracket of eq. (8) because of $n_2 \ll n_1$, and $I_{42}/I_{31} \approx (b_{42}/b_{31})\,(C_{14}/C_{13})$, as discussed above. On the other hand, in the Boltzmann regime, the second term is responsible for the intensity ratio as $I_{42}/I_{31} \approx (b_{42}/b_{31})\,(C_{24}/C_{13})\,(n_2/n_1)$ with a significant population of n_2 given by $n_1\,(g_2/g_1)\,e^{-E_{12}/kT_e}$. Because the energy difference between $^2P_{3/2}$ and $^2P_{1/2}$ of $2s^22p$ ground state is so small compared to the electron temperatures where Fe XXII is abundant, I_{42}/I_{31} reduces to $(g_2/g_1)\,(b_{42}/b_{31})\,(C_{24}/C_{13}) \approx 2\,(b_{42}/b_{31})\,(C_{24}/C_{13})$. On account of close excitation energies for C_{24} and C_{13} as seen in Fig. 4, the intensity ratio further reduces as $I_{42}/I_{31} \approx 2\,(b_{42}/b_{31})$. The small differences in the excitation energies for C_{13}, C_{14} and C_{24} are favorable to apply to density diagnostics with a weak electron temperature dependence. Also the close wavelengths of the resultant lines, 114 A and 117 A, have a practical advantage to be free from the wavelength-dependent sensitivities of the devices to observe.

Figs. 5 (a), (c) and (d) show the line intensity ratio of $2s^22p$ ($^2P_{3/2}$) - $2s2p^2$ ($^2P_{3/2}$) 114 A to $2s^22p$ ($^2P_{1/2}$) - $2s2p^2$ ($^2S_{1/2}$) 117 A observed for three plasma conditions,

ohmic and ICRF (ion cyclotron range of frequency) heating with gas puffing, ohmic heating with gas puffing and ohmic heating without gas puffing, respectively, for D/H gas discharges on the JIPP T-IIU tokamak. The ohmic heating is inherent and the others are operated at around 110-120 ms.[4] Fig. 5 (b) is the line-averaged electron density obtained by microwave interferometer for the condition of Fig. 5 (a). The line intensities observed in the earlier ohmic heating phase and in the later ohmic/ICRF heating phase are plotted with 1-σ error widths in Fig. 6. Here the density dependence of the line intensity ratio is drawn by more detailed calculations with 10 levels, and excitation by protons and deuterons as well as electrons is taken into account. The horizontal width of each error box represents the electron density at the plasma center by means of Thomson scattering.

4. General remarks

Radiative transition probability of hydrogenic ion is proportional to Z^4 for electric dipole transitions (E1), where Z is the nuclear charge, while the rate coefficient of collisional transition is proportional to Z^{-3} at a characteristic temperature T_e/Z^2 normalized to its hydrogenic ionization potential. Accordingly the density to satisfy a corona condition increases roughly in proportion to Z^7 with increasing the atomic number for optically allowed E1 transitions. For optically forbidden (non E1) lines, the critical density for the corona regime is lower than that for E1 because of their smaller transition probabilities. With increasing Z, the radiative transition probabilities for non E1 lines increase much faster than those for E1 lines as $A \propto Z^{6\text{-}10}$ with larger power of Z.

Fig. 7 (a) shows a schematic energy level diagram of He-like, Li-like and Be-like systems. Here we pick up the density dependence of the intercombination line (x,y) and the forbidden line (z) of He-like system. In the corona regime for 1s2s ($^3S_1$) state, excitation from the ground state $1s^2$ ($^1S_0$) of He-like ion and innershell ionization from the ground state $1s^22s$ ($^2S_{1/2}$) of Li-like ion is followed by forbidden transition z. With increasing the density, the collisional excitation to 1s2p (^3P) takes the place of radiative decay z in transition from 1s2s ($^3S_1$) and results in the intercombination lines x and y through the radiative decay from 1s2p (^3P). Then the relative intensity or the intensity ratio of the forbidden line z to the resonance line w decreases and that of intercombination

line increases, as seen in Fig. 7 (b).[5] As the density increases more, further excitation to 1s2p (^{1}P) by collisions takes the place of radiative decay x,y in transition from 1s2p (^{3}P) and results in the resonance line w. Thus, excitation to 1s2s ($^3S_1$) and 1s2p (^{3}P) is not followed by either z or x,y but ends in w via excitation to 1s2p (^{1}P) therefrom.

The critical density dividing the above regimes of the density dependence can be scaled as $n_e^C \propto Z^{14}$ with the atomic number, as seen in Fig. 7 (b) for oxygen and iron. This scaling is useful to see the range of applicability and the favorable elements for the density diagnostics. In He-like system there is another n=2 excited state 1s2s ($^1S_0$), which is stabilized by 2 photon decay into a continuum spectrum to the ground state of the same spin quantum number. Its radiative decay probability is smaller than that of 1s2s ($^3S_1$) and varies in proportion to Z^6. At densities considered here, transition from 1s2s ($^1S_0$) is dominated by further excitation to other n=2 states and results in the line spectra z, x,y or w depending on the density as discussed above.

Finally, we give a comment on nonequilibrium ionization. As shown in eq. (2), the transitions from/to level k affect the population of the levels 1 and 2, and are significant when the plasma deviates from an ionization equilibrium. In recombining, radiative recombination followed by cascade to lower levels plays an important role for the level population. Then the picture that excitation from the ground state is responsible for the level population fails, and the transitions from/to level k cannot be ignored. The level k here represents higher energy levels and the free electron state of only the ion A^{+z} concerned. Under ionizing conditions, the levels of the lower ionized $A^{+(z-1)}$ ion should be involved in eq. (2), because ionization from the levels of $A^{+(z-1)}$ may occur to populate directly the excited levels of A^{+z} without going by way of its ground state. This process is observed for O V in a tokamak plasma[2] and taken into account for the calculations of density dependence.[2,3] In nonequilibrium ionization, it should be noted that ionization/recombination processes from other ionic states can be more important for the population of excited levels than usual collisional excitation processes from the ground state. The transitions are no longer closed within an ionic state, but one has to solve the level population problem for all ionic states simultaneously. Then, the density dependence of line intensities is practically complicated though its principle based on competitive radiative and collisional transitions is kept alive.

References

1) Kato, T., Masai, K. and Mizuno, J., J. Phys. Soc. Japan 52, 3019, 1983.

2) Kato, T., Masai, K. and Sato, K., Phys.Lett. A 108, 259, 1985.

3) Kato, T., Lang, J. and Berrington, K.E., Atomic Data and Nuclear Data Tables 44, 133, 1990.

4) Masai, K. and Kato, T., Phys. Lett. A 123, 405, 1987.

5) Fujimoto, T. and Kato, T., private communication, 1990.

Figure Captions

Fig. 1 Schematic behavior of electron density dependence of line intensity ratio.

Fig. 2 Energy level diagram of Be-like oxygen (O V).

Fig. 3 Theoretical density dependence of line intensity ratios of $2s2p\ (^3P)$ - $2p^2\ (^3P)$ 760 A and $2s^2\ (^1S)$ - $2s2p\ (^3P)$ 1218 A to the resonance line $2s^2\ (^1S)$ - $2s2p\ (^1P)$ 760 A of O V. See text.

Fig. 4 Temperature dependence of rate coefficients for collisional excitation and energy level diagram of B-like iron (Fe XXII).

Fig. 5 Time variations of $2s^22p(^2P_{3/2})$ - $2s2p^2(^2P_{3/2})$ 114 A to $2s^22p(^2P_{1/2})$ - $2s2p^2(^2S_{1/2})$ 117 A of Fe XXII with (a) ohmic/ICRF heating and gas puffing, (c) ohmic heating and gas puffing and (d) ohmic heating, and (b) line-averaged electron density measured by microwave interferometer for the case (a). See text.

Fig. 6 Density dependence of the line intensity ratio $2s^22p(^2P_{3/2})$ - $2s2p^2(^2P_{3/2})$ 114 A to $2s^22p(^2P_{1/2})$ - $2s2p^2(^2S_{1/2})$ 117 A of Fe XXII calculated for excitation by (a) electrons, (b) electrons, deuterons and protons with densities $n_e/n_d/n_p$ = 1.0/0.9/0.1 and (c) electrons and protons with n_e/n_p = 1.0/1.0. The vertical and the horizontal widths of the box represent the errors of the observed intensity ratio and the electron density measured by Thomson scattering at the plasma center, repectively.

Fig. 7 (a) Energy level diagram for He-like, Li-like and Be-like systems and (b) electron density dependence of the intercombination line (x,y) and the forbidden line (z) to the resonance line (w) of He-like system for oxygen and iron.

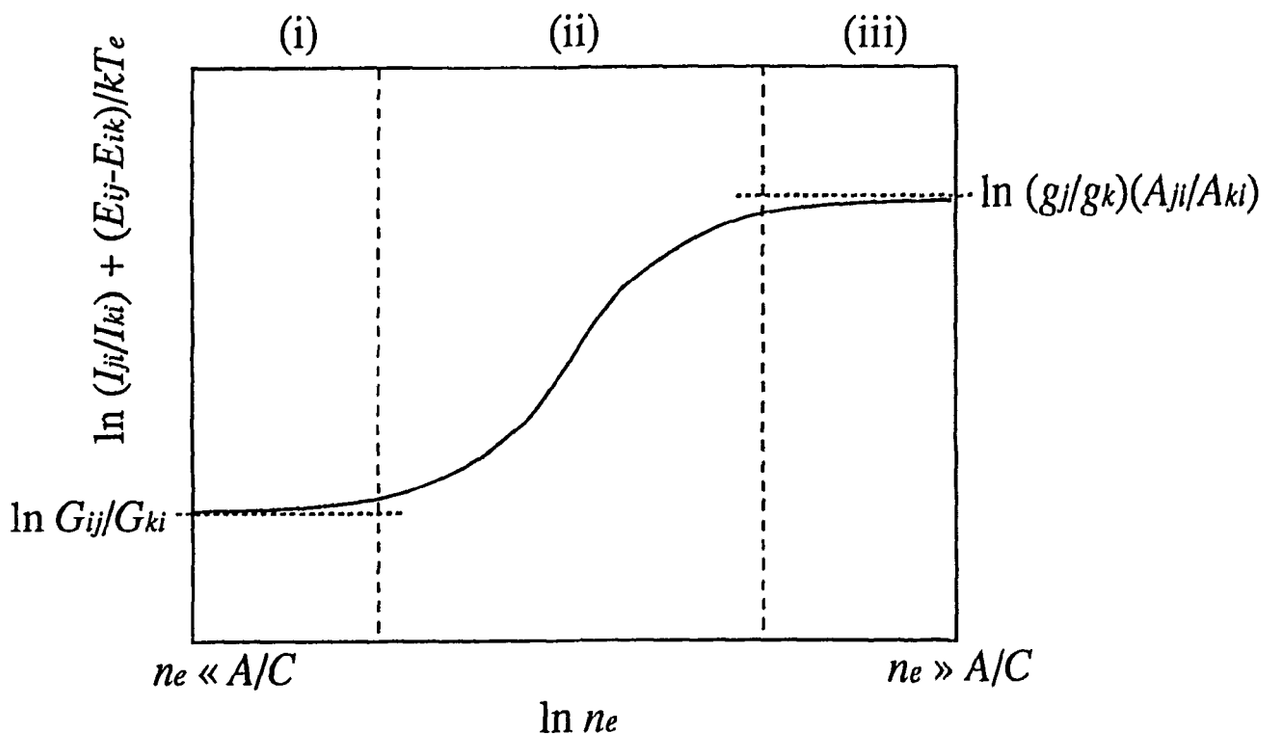
(i)
(ii)
(iii)
ln (Iji/Iki) + (Eij-Eik)/kTe
ln (gj/gk)(Aji/Aki)
ln Gij/Gki
ne « A/C
ne » A/C
ln ne

Fig.1

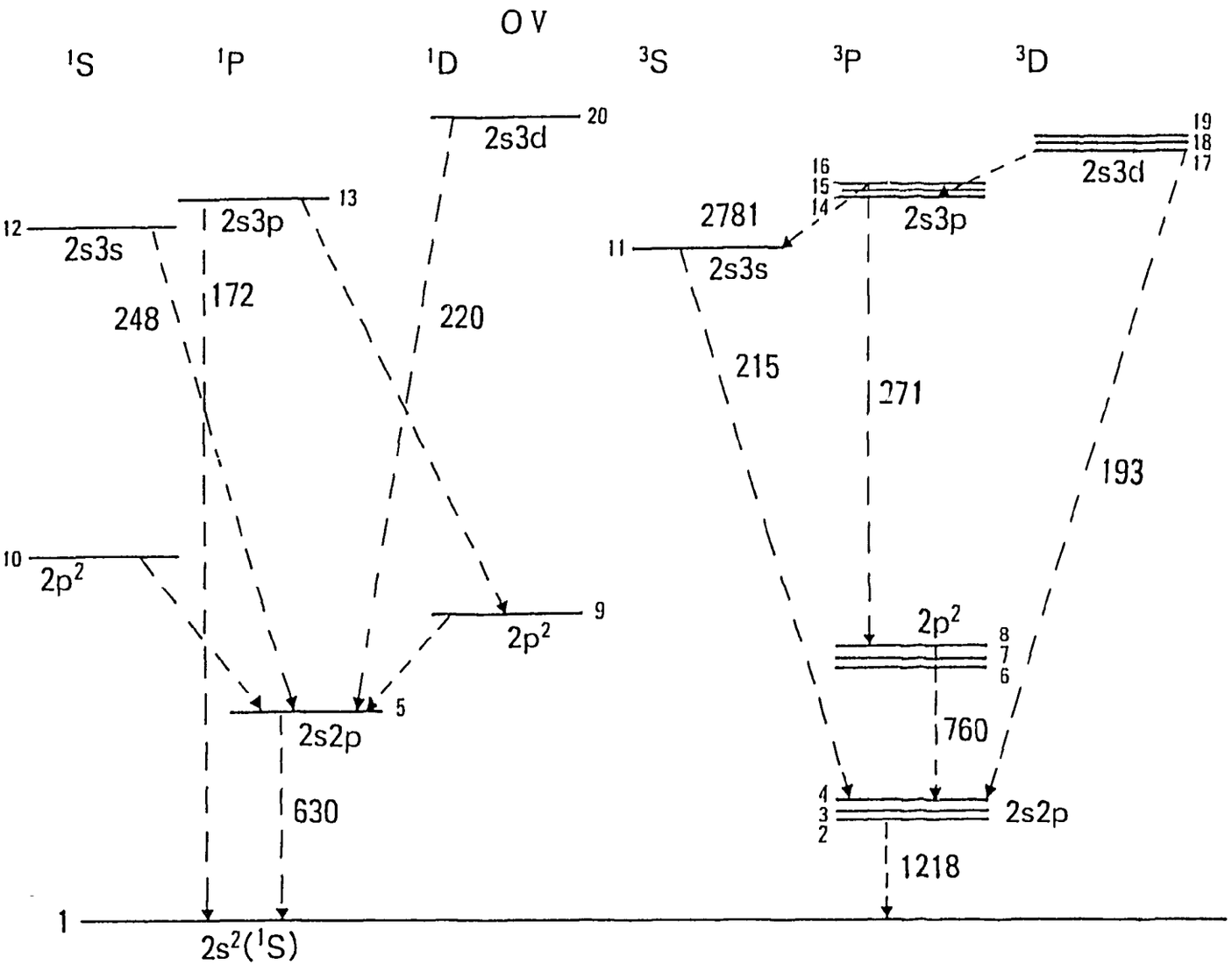
O V
1S
1P
1D
3S
3P
3D
20
2s3d
13
2s3p
12
2s3s
10
2p2
9
2p2
5
2s2p
1
2s2(1S)
248
172
220
630
19
18
17
2s3d
16
15
14
2s3p
2781
11
2s3s
215
271
193
2p2
8
7
6
760
4
3
2
2s2p
1218

Fig.2

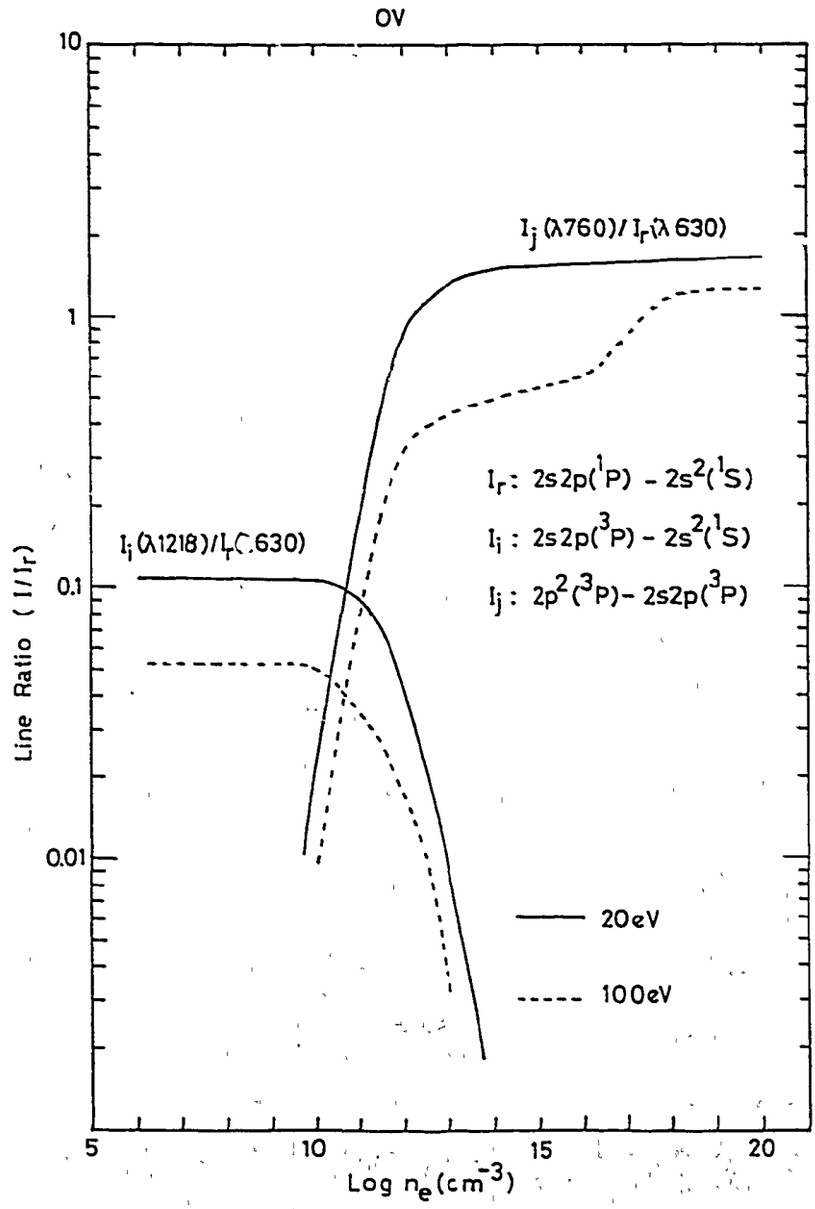
OV
10
1
0.1
0.01
I_j (λ760)/ I_r(λ 630)
I_i (λ1218)/I_r(λ630)
I_r: 2s2p(^{1}P) - 2s^2(^{1}S)
I_i : 2s2p(^{3}P) - 2s^2(^{1}S)
I_j : 2p^2(^{3}P)- 2s2p(^{3}P)
20eV
100eV
Line Ratio (I/I_r)
5
10
15
20
Log n_e(cm^{-3})

Fig.3 a

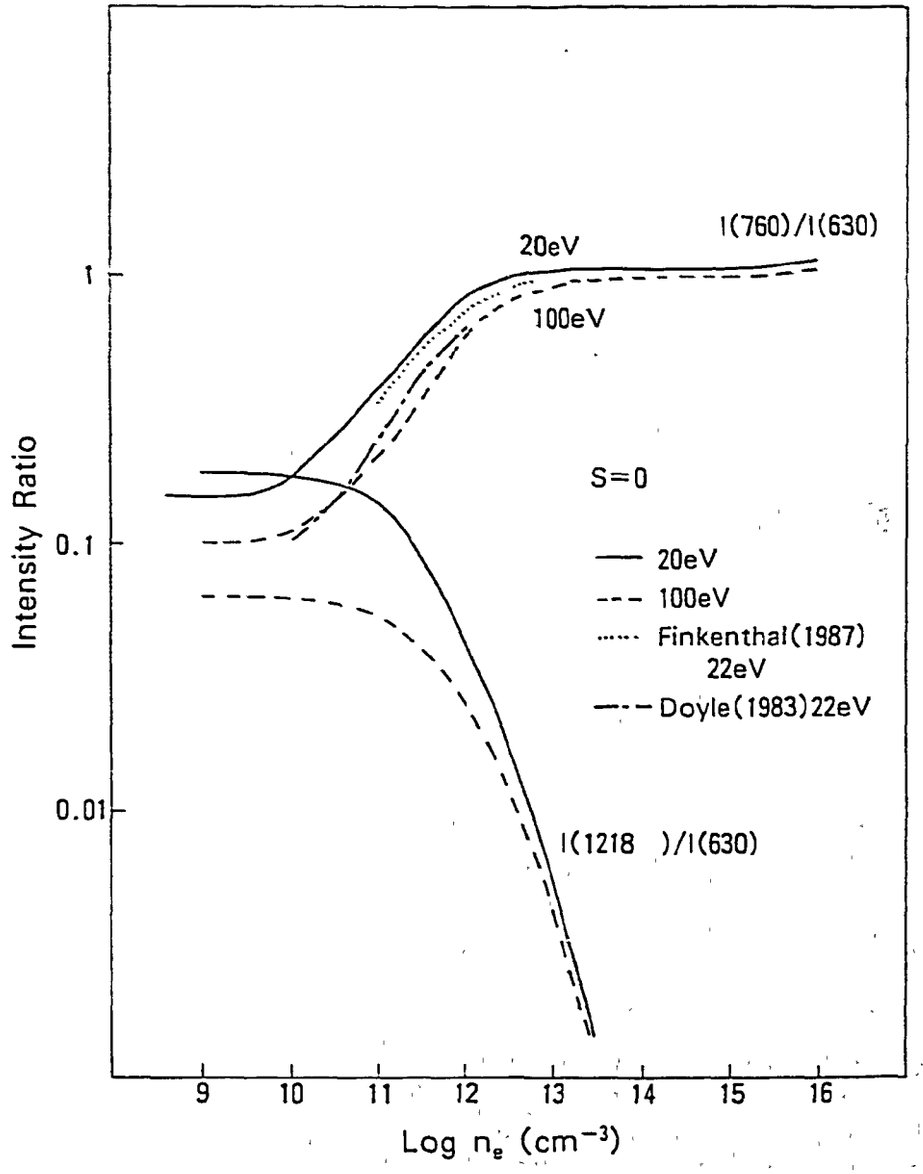
I(760)/I(630)
20eV
100eV
1
0.1
0.01
Intensity Ratio
S=0
20eV
100eV
Finkenthal(1987)
22eV
Doyle(1983)22eV
I(1218)/I(630)
9
10
11
12
13
14
15
16
Log n_e (cm^{-3})

Fig.3 b

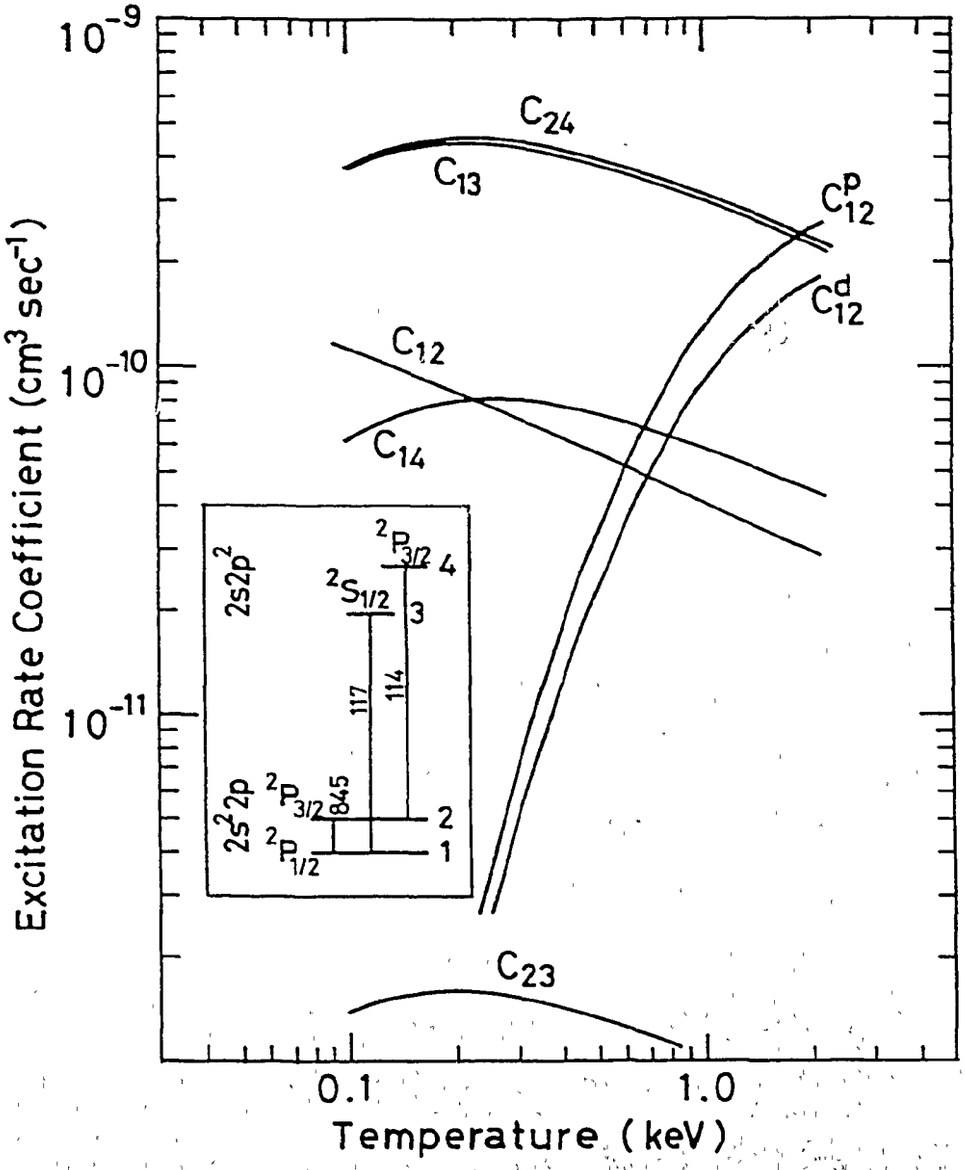
10^{-9}
10^{-10}
10^{-11}
Excitation Rate Coefficient ($cm^3\ sec^{-1}$)
C_{24}
C_{13}
C_{12}^{p}
C_{12}^{d}
C_{12}
C_{14}
C_{23}
$2s2p^2$
$^2P_{3/2}$ 4
$^2S_{1/2}$ 3
117
114
$2s^22p$
$^2P_{3/2}$
845
2
$^2P_{1/2}$
1
0.1
1.0
Temperature (keV)

Fig.4

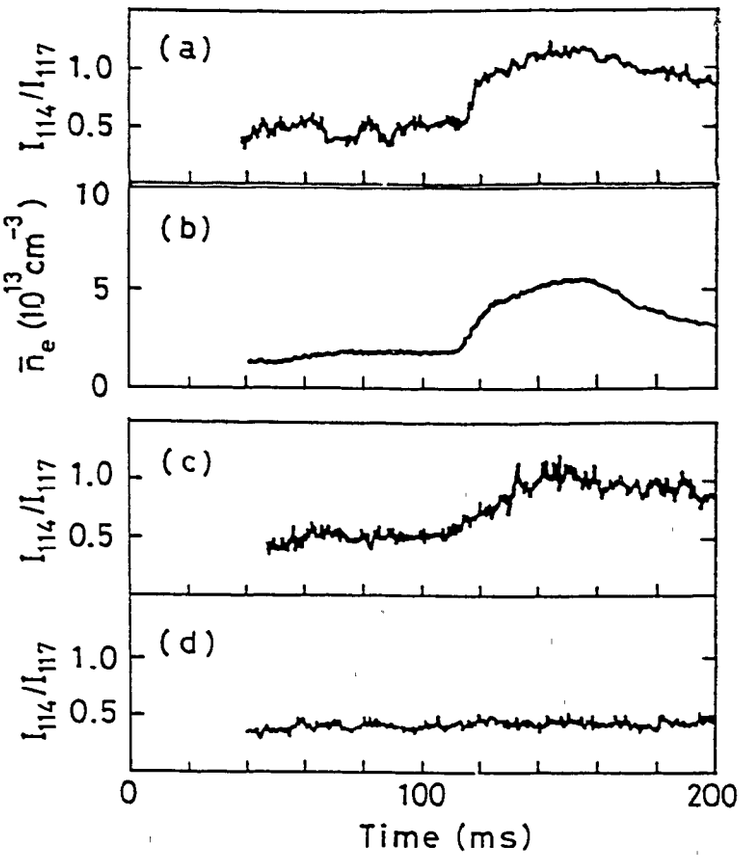

Fig.5

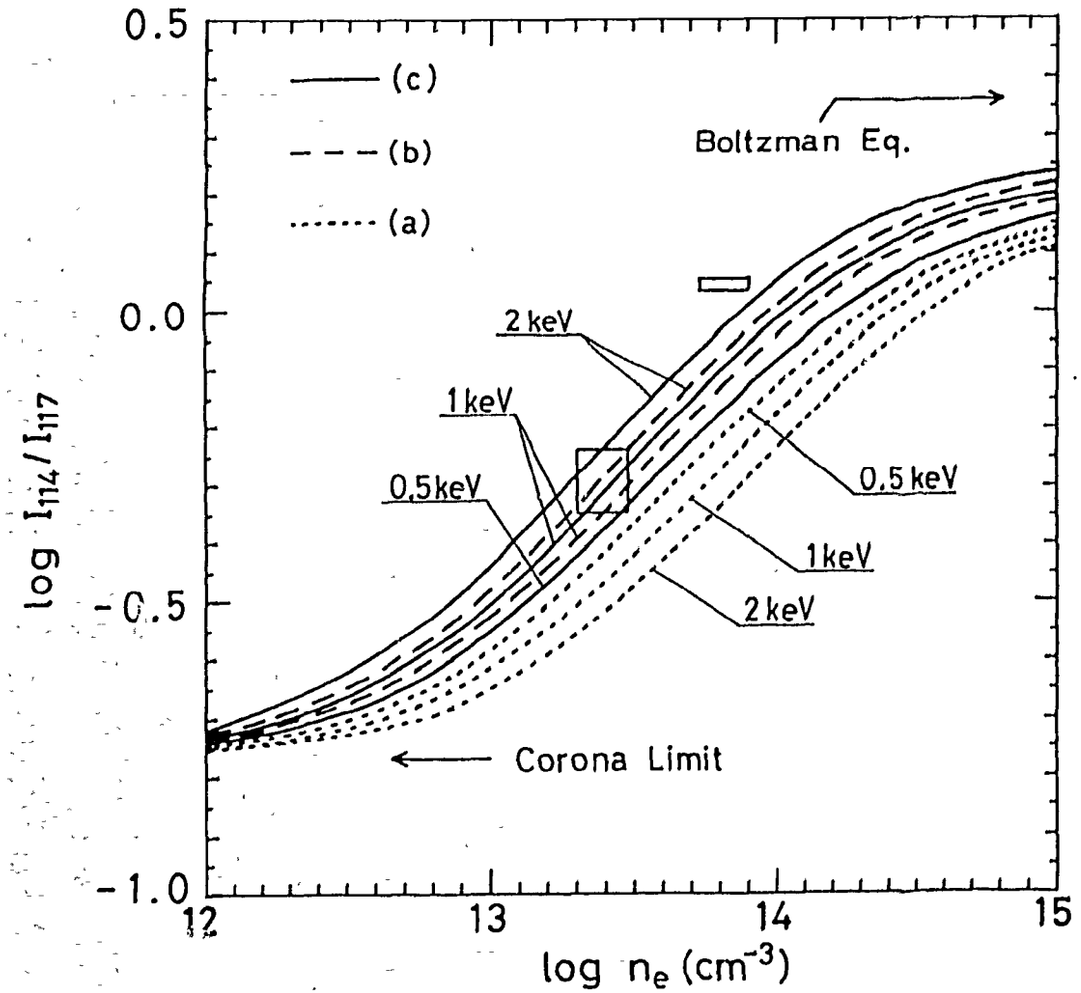
0.5
0.0
-0.5
-1.0
12
13
14
15
log I_{114}/I_{117}
log n_e (cm^{-3})
(c)
(b)
(a)
Boltzman Eq.
2 keV
1 keV
0.5 keV
0.5 keV
1 keV
2 keV
Corona Limit

Fig.6

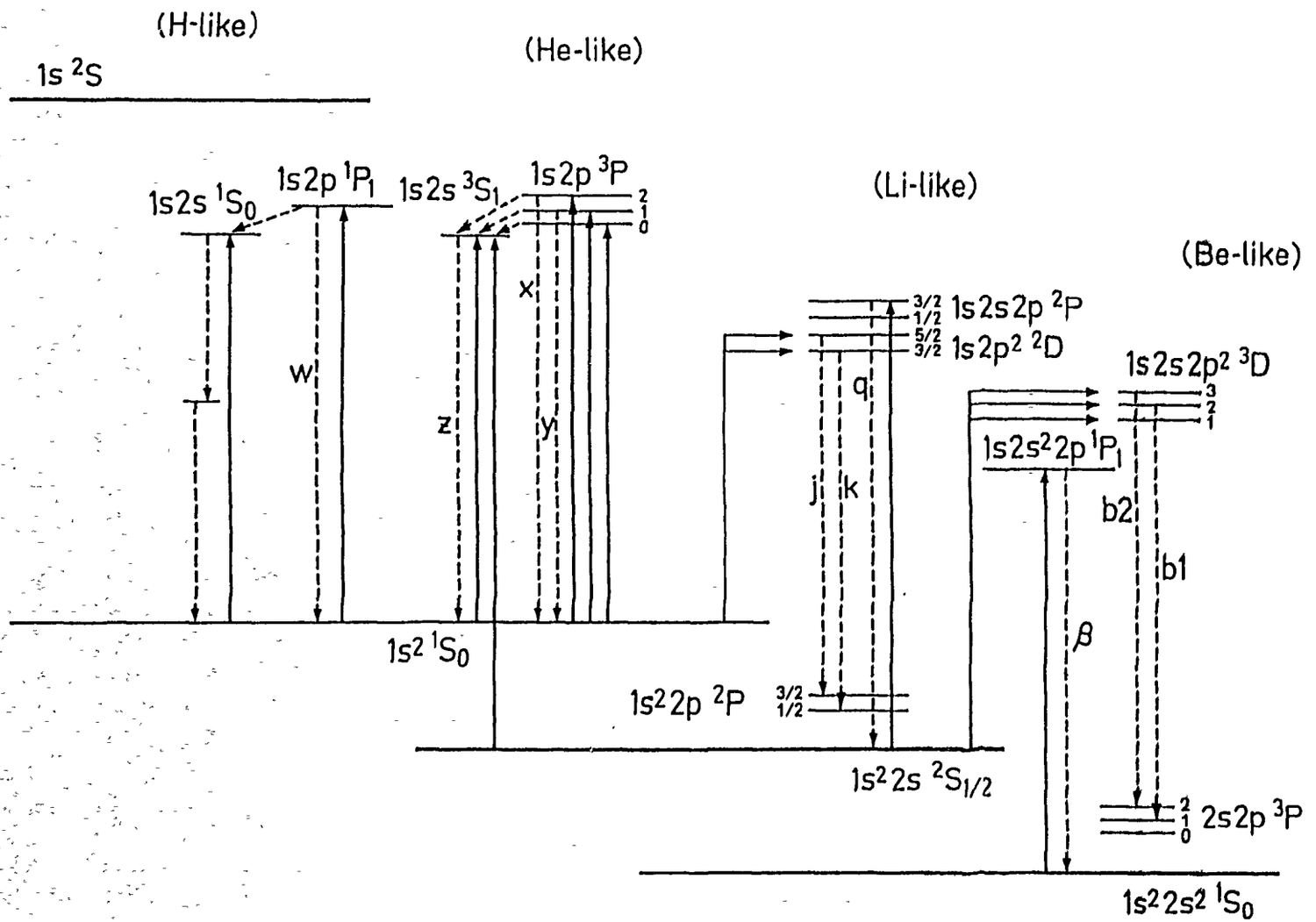
(H-like)
(He-like)
(Li-like)
(Be-like)
1s ²S
1s2s ¹S₀
1s2p ¹P₁
1s2s ³S₁
1s2p ³P
2
1
0
w
x
y
z
1s² ¹S₀
3/2 1s2s2p ²P
1/2
5/2 1s2p² ²D
3/2
q
j
k
1s2p ²P
3/2
1/2
1s² 2s ²S₁/₂
1s2s2p² ³D
3
2
1
1s2s²2p ¹P₁
b2
b1
β
2 2s2p ³P
1
0
1s² 2s² ¹S₀

Fig.7 a

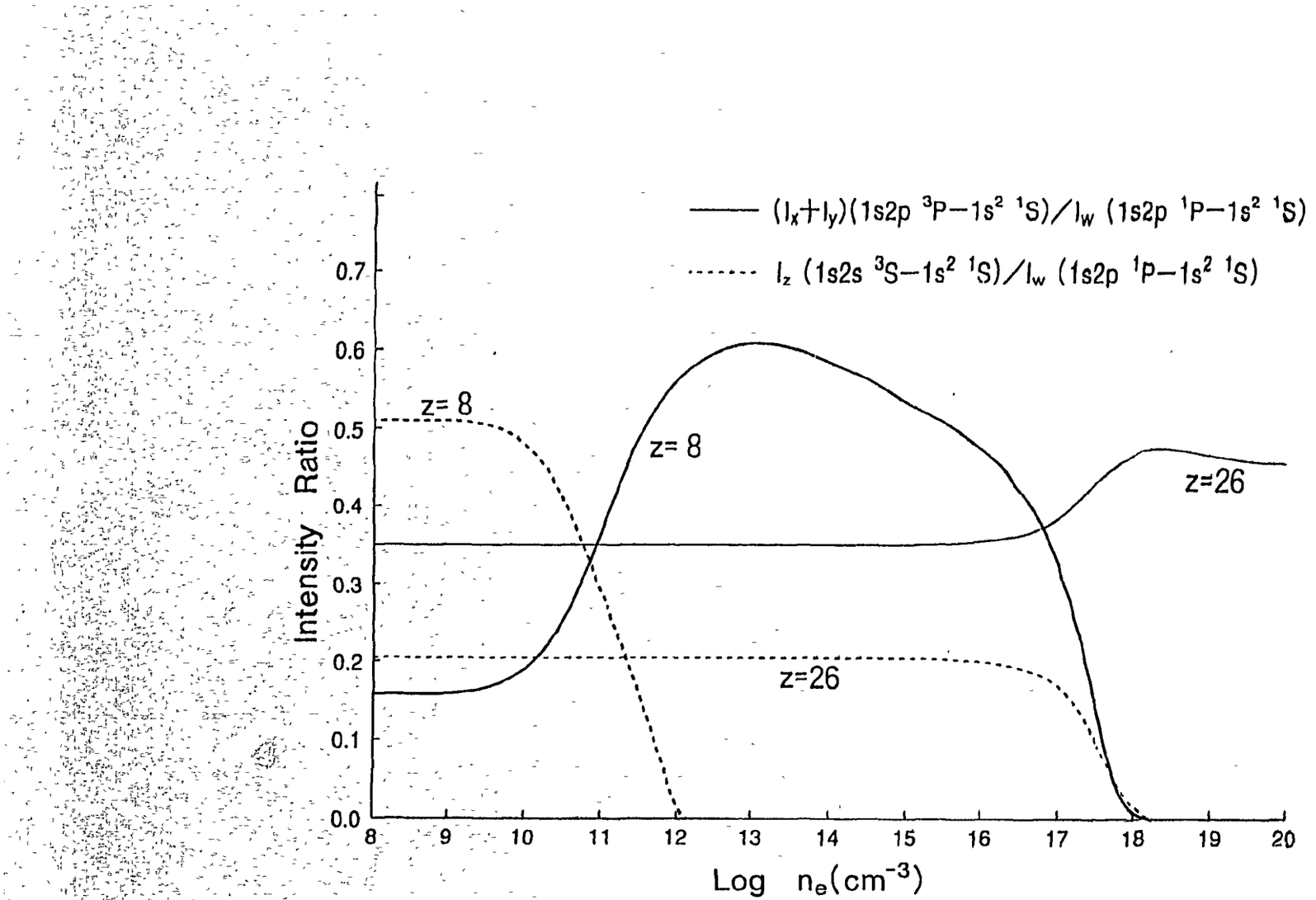
$(I_x+I_y)(1s2p\ ^3P-1s^2\ ^1S)/I_w\ (1s2p\ ^1P-1s^2\ ^1S)$
$I_z\ (1s2s\ ^3S-1s^2\ ^1S)/I_w\ (1s2p\ ^1P-1s^2\ ^1S)$
Intensity Ratio
0.0
0.1
0.2
0.3
0.4
0.5
0.6
0.7
z= 8
z= 8
z=26
z=26
8
9
10
11
12
13
14
15
16
17
18
19
20
Log $n_e(cm^{-3})$

Fig.7 b

Recent Issues of NIFS Series

NIFS-166 Vo Hong Anh and Nguyen Tien Dung, *A Synergetic Treatment of the Vortices Behaviour of a Plasma with Viscosity*; Sep. 1992

NIFS-167 K. Watanabe and T. Sato, *A Triggering Mechanism of Fast Crash in Sawtooth Oscillation*; Sep. 1992

NIFS-168 T. Hayashi, T. Sato, W. Lotz, P. Merkel, J. Nührenberg, U. Schwenn and E. Strumberger, *3D MHD Study of Helias and Heliotron*; Sep. 1992

NIFS-169 N. Nakajima, K. Ichiguchi, K. Watanabe, H. Sugama, M. Okamoto, M. Wakatani, Y. Nakamura and C. Z. Cheng, *Neoclassical Current and Related MHD Stability, Gap Modes, and Radial Electric Field Effects in Heliotron and Torsatron Plasmas*; Sep. 1992

NIFS-170 H. Sugama, M. Okamoto and M. Wakatani, *K- ϵ Model of Anomalous Transport in Resistive Interchange Turbulence* ; Sep, 1992

NIFS-171 H. Sugama, M. Okamoto and M. Wakatani, *Vlasov Equation in the Stochastic Magnetic Field* ; Sep. 1992

NIFS-172 N. Nakajima, M. Okamoto and M. Fujiwara, *Physical Mechanism of E_ψ-Driven Current in Asymmetric Toroidal Systems* ; Sep.1992

NIFS-173 N. Nakajima, J. Todoroki and M. Okamoto, *On Relation between Hamada and Boozer Magnetic Coordinate System* ; Sep. 1992

NIFS-174 K. Ichiguchi, N. Nakajima, M. Okamoto, Y. Nakamura and M. Wakatani, *Effects of Net Toroidal Current on Mercier Criterion in the Large Helical Device* ; Sep. 1992

NIFS-175 S. -I. Itoh, K. Itoh and A. Fukuyama, *Modelling of ELMs and Dynamic Responses of the H-Mode* ; Sep. 1992

NIFS-176 K. Itoh, S.-I. Itoh, A. Fukuyama, H. Sanuki, K. Ichiguchi and J. Todoroki, *Improved Models of β-Limit, Anomalous Transport and Radial Electric Field with Loss Cone Loss in Heliotron / Torsatron* ; Sep. 1992

NIFS-177 N. Ohyabu, K. Yamazaki, I. Katanuma, H. Ji, T. Watanabe, K. Watanabe, H. Akao, K. Akaishi, T. Ono, H. Kaneko, T. Kawamura, Y. Kubota, N. Noda, A. Sagara, O. Motojima, M. Fujiwara and A. Iiyoshi, *Design Study of LHD Helical Divertor and High Temperature Divertor Plasma Operation* ; Sep. 1992

NIFS-178 H. Sanuki, K. Itoh and S.-I. Itoh, *Selfconsistent Analysis of Radial Electric Field and Fast Ion Losses in CHS Torsatron / Heliotron* ; Sep. 1992

NIFS-179 K. Toi, S. Morita, K. Kawahata, K. Ida, T. Watari, R. Kumazawa, A. Ando, Y. Oka, K. Ohkubo, Y. Hamada, K. Adati, R. Akiyama, S. Hidekuma, S. Hirokura, O. Kaneko, T. Kawamoto, Y. Kawasumi, M. Kojima, T. Kuroda, K. Masai, K. Narihara, Y. Ogawa, S. Okajima, M. Sakamoto, M. Sasao, K. Sato, K. N. Sato, T. Seki, F. Shimpo, S. Tanahashi, Y. Taniguchi, T. Tsuzuki, *New Features of L-H Transition in Limiter H-Modes of JIPP T-IIU* ; Sep. 1992

NIFS-180 H. Momota, Y. Tomita, A. Ishida, Y. Kohzaki, M. Ohnishi, S. Ohi, Y. Nakao and M. Nishikawa, *D-^{3}He Fueled FRC Reactor "Artemis-L"* ; Sep. 1992

NIFS-181 T. Watari, R. Kumazawa, T. Seki, Y. Yasaka, A. Ando, Y. Oka, O. Kaneko, K. Adati, R. Akiyama, Y. Hamada, S. Hidekuma, S. Hirokura, K. Ida, K. Kawahata, T. Kawamoto, Y. Kawasumi, S. Kitagawa, M. Kojima, T. Kuroda, K. Masai, S. Morita, K. Narihara, Y. Ogawa, K. Ohkubo, S. Okajima, T. Ozaki, M. Sakamoto, M. Sasao, K. Sato, K. N. Sato, F.Shimpo, H. Takahashi, S. Tanahasi, Y. Taniguchi, K. Toi, T. Tsuzuki and M. Ono, *The New Features of Ion Bernstein Wave Heating in JIPP T-IIU Tokamak* ;Sep, 1992

NIFS-182 K. Itoh, H. Sanuki and S.-I. Itoh, *Effect of Alpha Particles on Radial Electric Field Structure in Torsatron / Heliotron Reactor*; Sep. 1992

NIFS-183 S. Morimoto, M. Sato, H. Yamada, H. Ji, S. Okamura, S. Kubo, O. Motojima, M. Murakami, T. C. Jernigan, T. S. Bigelow, A. C. England, R. S. Isler, J. F. Lyon, C. H. Ma, D. A. Rasmussen, C. R. Schaich, J. B. Wilgen and J. L. Yarber, *Long Pulse Discharges Sustained by Second Harmonic Electron Cyclotron Heating Using a 35GH$_Z$ Gyrotron in the Advanced Toroidal Facility*; Sep. 1992

NIFS-184 S. Okamura, K. Hanatani, K. Nishimura, R. Akiyama, T. Amano, H. Arimoto, M. Fujiwara, M. Hosokawa, K. Ida, H. Idei, H. Iguchi, O. Kaneko, T. Kawamoto, S. Kubo, R. Kumazawa, K. Matsuoka, S. Morita, O. Motojima, T. Mutoh, N. Nakajima, N. Noda, M. Okamoto, T. Ozaki, A. Sagara, S. Sakakibara, H. Sanuki, T. Seki, T. Shoji, F. Shimbo, C. Takahashi, Y. Takeiri, Y. Takita, K. Toi, K. Tsumori, M. Ueda, T. Watari, H. Yamada and I. Yamada, *Heating Experiments Using Neutral Beams with Variable Injection Angle and ICRF Waves in CHS* ; Sep. 1992

NIFS-185 H. Yamada, S. Morita, K. Ida, S. Okamura, H. Iguchi, S. Sakakibara, K. Nishimura, R. Akiyama, H. Arimoto, M. Fujiwara, K. Hanatani, S. P. Hirshman, K. Ichiguchi, H. Idei, O. Kaneko, T. Kawamoto, S. Kubo, D. K. Lee, K. Matsuoka, O, Motojima, T. Ozaki,

V. D. Pustovitov, A. Sagara, H. Sanuki, T. Shoji, C. Takahashi, Y. Takeiri, Y. Takita, S. Tanahashi, J. Todoroki, K. Toi, K. Tsumori, M. Ueda and I. Yamada, *MHD and Confinement Characteristics in the High-β Regime on the CHS Low-Aspect-Ratio Heliotron / Torsatron* ; Sep. 1992

NIFS-186 S. Morita, H. Yamada, H. Iguchi, K. Adati, R. Akiyama, H. Arimoto, M. Fujiwara, Y. Hamada, K. Ida, H. Idei, O. Kaneko, K. Kawahata, T. Kawamoto, S. Kubo, R. Kumazawa, K. Matsuoka, T. Morisaki, K. Nishimura, S. Okamura, T. Ozaki, T. Seki, M. Sakurai, S, Sakakibara, A. Sagara, C. Takahashi, Y. Takeiri, H. Takenaga, Y. Takita, K. Toi, K. Tsumori, K. Uchino, M. Ueda, T. Watari, I. Yamada, *A Role of Neutral Hydrogen in CHS Plasmas with Reheat and Collapse and Comparison with JIPP T-IIU Tokamak Plasmas* ; Sep. 1992

NIFS-187 K. Ioth, S.-I. Itoh, A. Fukuyama, M. Yagi and M. Azumi, *Model of the L-Mode Confinement in Tokamaks* ; Sep. 1992

NIFS-188 K. Itoh, A. Fukuyama and S.-I. Itoh, *Beta-Limiting Phenomena in High-Aspect-Ratio Toroidal Helical Plasmas*; Oct. 1992

NIFS-189 K. Itoh, S. -I. Itoh and A. Fukuyama, *Cross Field Ion Motion at Sawtooth Crash* ; Oct. 1992

NIFS-190 N. Noda, Y. Kubota, A. Sagara, N. Ohyabu, K. Akaishi, H. Ji, O. Motojima, M. Hashiba, I. Fujita, T. Hino, T. Yamashina, T. Matsuda, T. Sogabe, T. Matsumoto, K. Kuroda, S. Yamazaki, H. Ise, J. Adachi and T. Suzuki, *Design Study on Divertor Plates of Large Helical Device (LHD)* ; Oct. 1992

NIFS-191 Y. Kondoh, Y. Hosaka and K. Ishii, *Kernel Optimum Nearly-Analytical Discretization (KOND) Algorithm Applied to Parabolic and Hyperbolic Equations* : Oct. 1992

NIFS-192 K. Itoh, M. Yagi, S.-I. Itoh, A. Fukuyama and M. Azumi, *L-Mode Confinement Model Based on Transport-MHD Theory in Tokamaks* ; Oct. 1992

NIFS-193 T. Watari, *Review of Japanese Results on Heating and Current Drive* ; Oct. 1992

NIFS-194 Y. Kondoh, *Eigenfunction for Dissipative Dynamics Operator and Attractor of Dissipative Structure* ; Oct. 1992

NIFS-195 T. Watanabe, H. Oya, K. Watanabe and T. Sato, *Comprehensive Simulation Study on Local and Global Development of Auroral Arcs and Field-Aligned Potentials* ; Oct. 1992

NIFS-196 T. Mori, K. Akaishi, Y. Kubota, O. Motojima, M. Mushiaki, Y. Funato and Y. Hanaoka, *Pumping Experiment of Water on B and LaB_6 Films with Electron Beam Evaporator* ; Oct., 1992

NIFS-197 T. Kato and K. Masai, *X-ray Spectra from Hinotori Satellite and Suprathermal Electrons* ; Oct. 1992

NIFS-198 K. Toi, S. Okamura, H. Iguchi, H. Yamada, S. Morita, S. Sakakibara, K. Ida, K. Nishimura, K. Matsuoka, R. Akiyama, H. Arimoto, M. Fujiwara, M. Hosokawa, H. Idei, O. Kaneko, S. Kubo, A. Sagara, C. Takahashi, Y. Takeiri, Y. Takita, K. Tsumori, I. Yamada and H. Zushi, *Formation of H-mode Like Transport Barrier in the CHS Heliotron / Torsatron* ; Oct. 1992

NIFS-199 M. Tanaka, *A Kinetic Simulation of Low-Frequency Electromagnetic Phenomena in Inhomogeneous Plasmas of Three-Dimensions* ; Nov. 1992

NIFS-200 K. Itoh, S.-I. Itoh, H. Sanuki and A. Fukuyama, *Roles of Electric Field on Toroidal Magnetic Confinement*, Nov. 1992

NIFS-201 G. Gnudi and T. Hatori, *Hamiltonian for the Toroidal Helical Magnetic Field Lines in the Vacuum*; Nov. 1992

NIFS-202 K. Itoh, S.-I. Itoh and A. Fukuyama, *Physics of Transport Phenomena in Magnetic Confinement Plasmas*; Dec. 1992

NIFS-203 Y. Hamada, Y. Kawasumi, H. Iguchi, A. Fujisawa, Y. Abe and M. Takahashi, *Mesh Effect in a Parallel Plate Analyzer*; Dec. 1992

NIFS-204 T. Okada and H. Tazawa, *Two-Stream Instability for a Light Ion Beam -Plasma System with External Magnetic Field;* Dec. 1992

NIFS-205 M. Osakabe, S. Itoh, Y. Gotoh, M. Sasao and J. Fujita, *A Compact Neutron Counter Telescope with Thick Radiator (Cotetra) for Fusion Experiment*; Jan. 1993

NIFS-206 T. Yabe and F. Xiao, *Tracking Sharp Interface of Two Fluids by the CIP (Cubic-Interpolated Propagation) Scheme*, Jan. 1993

NIFS-207 A. Kageyama, K. Watanabe and T. Sato, *Simulation Study of MHD Dynamo : Convection in a Rotating Spherical Shell*; Feb. 1993

NIFS-208 M. Okamoto and S. Murakami, *Plasma Heating in Toroidal Systems*; Feb. 1993